

Experimental assessment of the effects of shade on an intertidal kelp: Do phytoplankton blooms inhibit growth of open-coast macroalgae?

Maria T. Kavanaugh¹

College of Oceanic and Atmospheric Sciences, Oregon State University, Corvallis, Oregon 97331

Karina J. Nielsen

Department of Biology, Sonoma State University, Rohnert Park, California 94928

Francis T. Chan, and Bruce A. Menge

Department of Zoology, Oregon State University, Corvallis, Oregon 97331

Ricardo M. Letelier

College of Oceanic and Atmospheric Sciences, Oregon State University, Corvallis, Oregon 97331

Lea M. Goodrich

Corvallis School District 509J, Corvallis, Oregon 97333

Abstract

Benthic primary producer abundance and satellite-derived chlorophyll concentrations are strongly negatively correlated along the Oregon and Northern California coast, suggesting an antagonistic interaction. Direct field observations of interannual and among-site changes in abundance of low intertidal macrophytes also suggest a negative interaction. Several years (2001–2006) of quantification of surf-zone chlorophyll concentrations and light reaching the intertidal benthos suggested that severe light attenuation from dense phytoplankton blooms is an important mechanism underlying this inverse phytoplankton–macrophyte relationship. From early June to September of 2004 we quantified the response of the intertidal kelp *Saccharina sessile* to experimentally manipulated light regimes that mimicked the attenuation during blooms. Shading frames were installed in the low intertidal zone to manipulate the light levels available to the benthos at two sites of contrasting long-term differences in average phytoplankton abundance. Treatments included shaded and unshaded plots that were 0.25 m² in area. Although the magnitude of the effect was context-dependent, shading strongly decreased growth rates and abundance of *S. sessile*. These results are comparable to results in estuarine studies that have demonstrated adverse effects on benthic macrophytes as a result of eutrophication and subsequent light limitation and are the first demonstration of phytoplankton-induced light limitation for energetic open coasts. In these systems where annual benthic production can exceed the pelagic production and where perennial macrophytes such as kelp and surf grasses are important habitat modifiers, large-scale reduction of macrophytes via phytoplankton shading could lead to profound modifications of coastal ecosystem dynamics.

¹ Corresponding author (mkavanau@coas.oregonstate.edu).

Acknowledgments

We thank J. Lubchenco, A. Milligan, and K. Milligan for their intellectual contributions and two anonymous reviewers for their generous comments in improving this manuscript. We also thank J. Flitcroft, K. Haggard, J. Nahorniak, W. Wood, and the Partnership for Interdisciplinary Studies of Coastal Oceans (PISCO) technicians, undergraduate, and graduate students for their untiring logistical and engineering support, and B. Abbott for access to the Fogarty Creek site. The script for parameterizing photosynthesis vs. irradiance curves for PAM data was written by A. E. White.

This project was partially funded by a Mamie Markham Graduate Research Award from the Hatfield Marine Science Center and NASA ESS fellowship NNX07A032H to M.T.K.; grants from the David and Lucile Packard Foundation, the Gordon and Betty Moore Foundation, the Wayne and Gladys Valley Foundation, and the Andrew Mellon Foundation to B.A.M. and Jane Lubchenco; NSF grant OCE-0726983 to B.A.M., K.J.N., F.C., and Sally Hacker; and NSF grant OCE-0435619 to R.M.L., Timothy Cowles, Jack Barth, and Yvette Spitz.

This is contribution number 302 from PISCO, funded primarily by the Gordon and Betty Moore Foundation and the David and Lucile Packard Foundation.

Models of global warming and increased anthropogenic alteration of biogeochemical cycles generally predict marked changes in phytoplankton primary production and abundances in the coastal ocean (Justic et al. 1996; Boyd and Doney 2002). Models of oceanographic regime shift (e.g., El Niño Southern Oscillation, Pacific Decadal Oscillation) also focus on changes in planktonic-based production and abundance (Mantua et al. 1997); when changes in phytoplankton abundances occur, the resultant alteration of “bottom-up” effects are of great potential importance to coastal marine ecosystems (e.g., Bustamante et al. 1995; Menge et al. 1997). With higher phytoplankton concentrations, for example, growth and survival of planktotrophic larvae and filter-feeding sessile invertebrates seem likely to increase (Phillips 2005; Menge et al. 2008), with resultant changes in interaction strengths and community structure (Menge et al. 1996). Another potential consequence of phytoplankton blooms, the effects of shading on benthic macrophyte communities, is poorly known in energetic, open-coast systems.

Benthic macrophyte assemblages are critical to biogeochemical cycles and ecological interactions. Open-coast systems can often support net benthic primary production of over $1000 \text{ g C m}^{-2} \text{ yr}^{-1}$ (Borum and Sand-Jensen 1996). In these regions, annual net primary production (m^{-2}) of perennial kelps and sea grasses can be 5 (Borum and Sand-Jensen 1996) to 10 times (Mann 1972) greater than that of phytoplankton. Kelps also have important roles as ecosystem engineers (Jones et al. 1994) and provide nursery habitat for commercially important fish and invertebrates (Mann 1972; Steneck et al. 2002). A shift in dominance from benthic macrophytes to phytoplankton not only would have profound ecological effects but also may reduce the productivity of coastal ecosystems.

Previous studies in estuaries demonstrate the potential of phytoplankton to outcompete macroalgae and seagrasses for light, resulting in dramatic shifts in benthic macrophyte assemblages (Lavery et al. 1991; Valiela et al. 1997), especially in eutrophic conditions and where residence times of water are high. In high-energy, open-coast systems, the potential for phytoplankton shading to stunt intertidal macrophyte growth has been generally thought to be limited (Dring 1987). However, recent measurements of light attenuation along the upwelling-dominated central Oregon coast have been extraordinarily high during summer phytoplankton blooms (i.e., July 2001: $K_d = 1.7\text{--}3$; Nielsen et al. unpubl.). Because photosynthesis of intertidal algae may be curtailed during emersion (Williams and Dethier 2005), there is the potential for bio-optical properties in the water column to affect algal-dominated communities even in energetic intertidal regions of open coast.

Here we present the results of three analyses. First, we investigate the regional patterns of abundance of benthic macrophytes and nearshore phytoplankton. Second, we examine the patterns of abundances of these primary producers over 5 yr in two regions that, despite similar upwelling dynamics, have historically varying phytoplankton standing stock. Third, we report the results of a manipulative field experiment in which we tested the hypothesis that the growth rate of the low intertidal kelp *Saccharina sessile* (formerly *Hedophyllum sessile* Setchell; Lane et al. 2006) is limited by light availability during summer blooms along the Oregon coast. We used a combination of modeling, experimental manipulation, and in situ measurements of frond elongation and relative abundance of *S. sessile* under different light regimes at two sites with persistently different phytoplankton abundances. After establishing an ecologically relevant range of light attenuation, we focus on the following questions: (1) what is the influence of reduced light intensity on variation in kelp growth and abundance? and (2) how does this effect vary through space and time?

Methods

Regional and temporal context—Satellite ocean color imagery from the Sea-viewing Wide Field-of-view Sensor (SeaWiFS) was used to establish the spatiotemporal context of phytoplankton standing stock. Standard level

3-mapped derived chlorophyll *a* (Chl *a*) concentrations and integrated photosynthetically active radiation (PAR) were downloaded (<http://oceancolor.gsfc.nasa.gov/>), and a time or space series was constructed from the nearest visible pixel adjacent (due west) to sites where macrophyte abundance had been previously assessed. Low-zone intertidal macroalgal abundance was quantified in a spatially nested design using the transect quadrat method described in Schoch et al. (2006). For our analysis, total macrophyte cover was determined as the sum of individual species' cover per quadrat; because both understory and canopy percentage cover were estimated, total cover could exceed 100%. Quadrat-level data were averaged to the transect level and then transect-level averages were reported for each site ($n = 3$).

To quantify the relationship between macrophyte abundance and phytoplankton concentration, we conducted two separate linear regression analyses using macrophyte abundance and satellite-derived Chl *a* data described above. The first analysis explored the relationship between benthic macrophyte abundance and mean summer Chl *a* concentrations for a single year (2002) at several sites along the west coast of the U.S. (Table 1; Fig. 1). The second comparison focused on changes in Chl *a* and benthic macrophyte abundance over time at two sites: Fogarty Creek (FC) and Strawberry Hill (SH) (further described in next section). Eight-day composites of satellite-derived Chl *a* concentrations were binned into a single "annual" mean for May through July for each year (1998–2006) to correspond with the general timing of macrophyte surveys. Macrophyte data were available only from 2000 to 2004; therefore, the temporal comparison of macrophyte abundance as a function of Chl *a* is constrained to 5 yr.

Field experiment—Study sites: The field experiment was conducted at two sites on the central Oregon coast: FC (44.84°N , 124.05°W), a site on Cape Foulweather, and SH (44.24°N , 124.11°W), a site on Cape Perpetua (Fig. 1). These sites have similar patterns of upwelling and macronutrient concentrations (Menge et al. 1997) yet different levels of phytoplankton standing stock (Menge et al. 1997; Leslie et al. 2005). The sites are also characterized by differences in relative abundances of sessile invertebrates and macrophytes. FC has high relative abundances of macroalgae and low relative abundances of sessile filter feeders such as barnacles and mussels. The reverse is true for SH (Menge et al. 1997).

Field observations taken during 15+ yr of intensive field studies have demonstrated that the two sites also differ in several physical parameters. Air temperatures tend to be slightly higher at SH (Menge et al. 1997; Halpin et al. 2004); sand deposition is high at SH (Trowbridge 1996; Menge et al. 1997) and low at FC. Furthermore, the continental shelf is wider at SH and could facilitate greater larval and or phytoplankton retention (Menge et al. 1997). Here, the upwelling front can move offshore, allowing for seasonal recirculation of water (Kirincich et al. 2005), and thereby providing a physical mechanism for retention of water and subsequent accumulation of phytoplankton biomass.

Table 1. Sites included in regional analysis comparing satellite-derived [Chl *a*] and benthic macrophyte abundance (% cover). See Fig. 1.

Site Name	Latitude (°N)	Longitude (°W)
Ecola Point	45.92	123.98
Cape Falcon	45.77	123.98
Smugglers Cove	45.76	123.97
Fogarty Creek and Boiler Bay	44.83	124.06
Depoe Bay	44.81	124.06
Otter Crest	44.75	124.07
Strawberry Hill	44.25	124.11
Tokatee Klootchman	44.20	124.12
Qochyax Island	43.33	124.38
Cape Arago	43.31	124.41
Trinidad Head	41.07	124.16
Kibesillah Hill	39.60	123.79
Todd Point	39.42	123.82
Point Cabrillo Lighthouse	39.35	123.83
Van Damme State Park	39.28	123.80
Mussel Point	38.32	123.08
Horseshoe Cove	38.32	123.07
Point Lobos	36.52	121.95
Malpasos Creek	36.48	121.94
Soberanes Point	36.45	121.93

Modeling the intertidal light environment: Because carbon limitation may constrain photosynthesis by intertidal macroalgae during emersion (e.g., Williams and Dethier 2005), three factors control the effective daily dose of PAR: the length of time immersed, the downwelling intensity of PAR during immersion, and the attenuation of PAR during immersion by the overlying water column. To determine an ecologically relevant level of shading, we modeled PAR, mean water depth, and attenuation over a complete spring tidal cycle (early July 2001).

The downwelling light available to the low intertidal during high phytoplankton biomass was modeled using the Beer-Lambert Law:

$$E_z = E_0 e^{-K_{dPAR}z} \quad (1)$$

where E_z is the modeled irradiance at the benthos. E_0 is the modeled surface irradiance using a 16-h day length imposed on a Gaussian-like light intensity curve (maximum = $2000 \mu\text{mol m}^{-2} \text{s}^{-1}$ at 12:00 h). K_{dPAR} is the average attenuation coefficient previously measured for central Oregon coast sites during bloom conditions ($1.7\text{--}3.0 \text{ m}^{-1}$; Nielsen et al., unpubl.), and z is the tidally modulated depth of the water column above the *S. sessile* zone calculated as the difference between the tidal height of the *S. sessile* zone (1 m below mean sea level; M. T. Kavanaugh unpubl.) and the predicted tidal height from an existing tidal model (Tides and Currents, 1999, Nobeltec). Converting the range of attenuation to time-integrated transmittance ($E_z:E_0$ over the ~ 14 -d spring tide cycle) suggests that only 28–39% of the mean diel incident irradiation was transmitted and therefore available to the benthos along the Oregon coast. Considering only times during immersion, these values fell to 12–26%. We do not know the degree to which

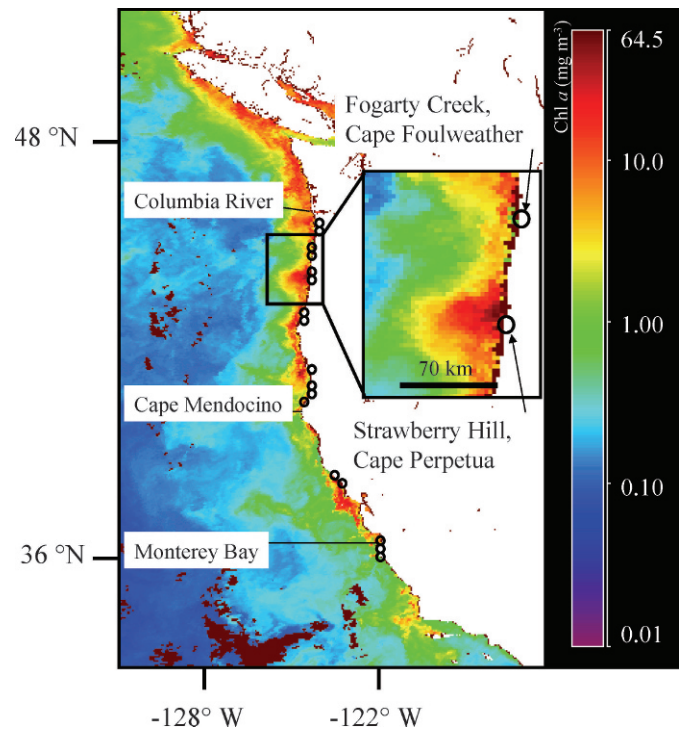


Fig. 1. Map of region of U.S. west coast highlighting region of interest on the central Oregon coast with field sites, SH (44.24°N , 124.11°W) and FC (44.84°N , 124.05°W). The linear distance between sites is approximately 70 km. Open circles denote sites included in regional comparison of satellite-derived [Chl *a*] and benthic macrophyte abundances. Points of spatially proximal sites may overlap on the figure.

photosynthesis in *S. sessile* is curtailed during emersion; the more conservative values were used to determine the level of experimental shading described in the light manipulation section below.

To put the transmissivity of the shades into historical and broader ecological context, we modeled transmissivity over a range of Chl *a* concentrations using a static, empirical, chlorophyll-specific attenuation coefficient (k_c). Light attenuation by phytoplankton (K_{phyto}) is dependent on phytoplankton biomass (B_c ; often expressed as [Chl *a*]) and the specific vertical attenuation (k_c) per unit of phytoplankton (Morel 1988):

$$K_{\text{phyto}} = B_c \times k_c \quad (2)$$

Morel (1988) reports a dynamic k_c for blue water that decreases exponentially with [Chl *a*] because of self-shading or packaging of pigments within the cell ($0.2\text{--}0.007 \text{ m}^2 \text{ mg Chl } a^{-1}$). However, the Morel equation has been validated only for Chl *a* concentrations up to 30 mg m^{-3} ; surf-zone Chl *a* concentrations along the Oregon coast have reached levels at least five times that (Grantham et al. 2004). In this analysis we used a static estimate of k_c to represent the relatively shallow and well-mixed surf zone that overlies intertidal habitats, because our empirical estimate of k_c was best described as a linear relationship between K_{dPAR} and

Chl *a* concentration (Kirk 1994). We empirically derived k_c from measured attenuation of PAR and extracted Chl *a* (Nielsen et al. unpubl.) from four sites along the central and southern Oregon coast during the period of 09 July–30 August 2001. Binning daily values to 7-d averages, the following relationship was determined:

$$K_d(\text{PAR}) = 0.785 + 1.16\log_{10}[\text{Chl } a], \quad (3)$$

$$(R^2 = 0.65, F_{1,12} = 20.7, p = 0.001)$$

Using the slope of Eq. 3 to solve for Eq. 2, we derive a $k_c = 0.02 \text{ m}^2 \text{ mg Chl } a^{-1}$, a value within the range of values reported by previous investigators. In a meta-analysis of over 400 temperate fresh and marine waters, Krause-Jensen and Sand-Jensen (1998) reported static $k_c = 0.004\text{--}0.029 \text{ m}^2 \text{ mg Chl } a^{-1}$, and Kirk (1994) reported $k_c = 0.016 \text{ m}^2 \text{ mg Chl } a^{-1}$ for mixed assemblages in various oceanic and coastal waters. Furthermore, because the downward attenuation of light is described as the sum of attenuation by water, dissolved organic matter (DOM), detritus, and phytoplankton (Kirk, 1994), the single-variable equation in Eq. 3 assumes that K_{phyto} is the dominant term in controlling variations in K_d or that K_{phyto} is a reasonable proxy for K_{DOM} and K_{detritus} in phytoplankton-rich coastal waters where phytoplankton-derived organic materials dominate particulate and dissolved organic carbon pools over weekly time scales. Replacing K_{dPAR} in Eq. 1 with our empirically derived K_{phyto} and solving for $E_z:E_0$ at 1-m depth, we modeled the transmission of light to the *S. sessile* zone over a range of Chl *a* concentrations.

Photosynthetically usable radiation and spectral overlap: Phytoplankton absorb light of different spectral qualities, thereby altering the photosynthetically usable radiation reaching the benthos (Sullivan et al. 1984). Although diatoms and kelps may be expected to have similar absorption spectra because of phylogenetic similarities of chlorophyll types and accessory pigments (e.g., fucoxanthin), the relative absorption by accessory pigments as compared to Chl *a* may vary, as can the dominance of diatoms in the phytoplankton assemblage. To determine the effect of coastal phytoplankton on light quality, we compared the relative absorbance capacity of *S. sessile* to that of a common coastal diatom (*Thalassiosira weissflogii*) in culture, and to a mixed phytoplankton assemblage from nearshore waters along the Oregon coast. Because in situ phytoplankton samples were not specifically collected for spectral qualities during the experiment, we used information gathered previously (June 2001, 44.42°N, 124.16°W; Letelier, unpubl.). 50-mL seawater samples were filtered onto a 25-mm glass fiber filter and frozen in liquid nitrogen for later extraction. *S. sessile* tissue samples ($n = 10$) were collected in April 2004 from SH only, frozen in liquid nitrogen in the field, and stored in the lab at -80°C for later analysis. All samples were extracted in 15 mL high-performance liquid chromatography-grade acetone in the dark for 48 h at -15°C ; absorbance spectra were analyzed using a CARY Bio-300 UV visible spectrometer. Each

spectrum was normalized to its individual maximal absorbance.

Manipulating the light available to *S. sessile*: The use of shaded plots in field experimentation has been effective in isolating temperature and light effects in rocky intertidal habitats (Harley 2002; Burnaford 2004). To manipulate light input to *S. sessile*, shades covering $50 \times 50\text{-cm}$ plots were installed in the lower intertidal zone. Shades were designed by attaching Vexar® mesh (4-mm mesh size, neutral spectral density) to a stainless steel frame. Stainless steel all-thread supports were inserted approximately 15 cm into holes drilled into the bedrock, and cemented into the holes with marine epoxy (Z*SPAR, Kop-Coat). The shading mesh was elevated approximately 20 cm over the rock surface. The goal of the design was to block an ecologically relevant percentage of the light and to provide a structure that would resist wave action and allow ample water flow. To minimize potential alteration of flow by the mesh, shades were not extended down the sides of the supports. PAR values were determined using a hand-held quantum meter (Model QSX-01, Apogee) during a period of emersion. Shades transmitted between 25% and 40% of PAR at the center of the plot. Because these measurements were conducted in late morning and did not incorporate low sun angles, daily integrated transmissivities were likely higher. The experiment was monitored biweekly; during monitoring, the few torn shades were repaired and fouling organisms were removed. Thus, the relative percentage of light blocked remained fairly constant through the duration of the experiment.

We monitored the growth and abundance of *S. sessile* under experimentally manipulated light conditions over the course of a growing season, early June–September 2004. We focused on *S. sessile* for the growth measurements because it is a competitive dominant (Paine 1984; Dayton 1985), and has high relative abundance ($\sim 45\text{--}100\%$ cover, this study) in the low zone at both FC and SH. Like other kelps, *S. sessile* is also likely to experience increased growth during the upwelling season, a time when increased nutrient supply can also trigger dense phytoplankton blooms in coastal waters. *S. sessile* is a biennial kelp that grows in two sporophyte morphologies: a bullate morph prevalent in sheltered habitats and a strap-like morph prevalent in wave-exposed habitats (Armstrong 1989). We focused on first-year sporophytes of the latter morphology for the growth measurements. To quantify growth rates, a 3-mm hole was punched 5 cm from the base (to avoid damaging the meristem) during each visit (Kain 1976; Larkum 1986). Growth was calculated as the mean difference between the previous hole and the new hole.

We haphazardly set up plots centered over *S. sessile* thalli through the middle of the *S. sessile* zone at each site. All plots faced approximately west; mean elevation of plots did not differ between sites and ranged from 0.94 to 1.05 m below mean sea level. Three treatments were applied: an artificially shaded plot in which *S. sessile* blades were trimmed to 15 cm to avoid abrasion effects of the mesh on the kelp blades (+shade, +trim), a non-shaded

control (–shade, +trim) in which plots were marked and *S. sessile* was trimmed to 15 cm, and an unmanipulated reference plot (–shade, –trim) that controlled for trimming. Blades in the +trim treatments were re-trimmed to 15 cm during each visit. A +shade, –trim plot was not included in the design because the measurement of growth would likely be confounded by abrasion effects. Each treatment had five replicates, for a total of 15 plots per site. Several (4–5) *S. sessile* fronds were subsampled in each plot to increase precision; variance in elongation was quantified at the plot level. To monitor changes in abundance at both sites, percentage cover and density of *S. sessile* were quantified during each visit using visual estimates (Dethier et al. 1993).

Physiologically, light limitation is defined as the decrease in photosynthesis or growth caused by reducing available PAR from saturating to subsaturating irradiances. At the end of the experiment (mid-September 2004), photosynthesis vs. irradiance curves were assessed using a diving pulse-amplitude modulated (PAM) fluorometer (Heinz Walz GmbH) to determine the range of subsaturating irradiances for *S. sessile*. Because light history can affect the quantum yield of fluorescence in kelps on scales of a few hours (Nielsen et al. 2006), blades from unmanipulated plots ($n = 5$) at both sites were brought into the lab and dark-adapted in artificial seawater at 8°C for 24 h prior to measurement. Leaf clips were attached in the dark and rapid light curves (Genty et al. 1989; Falkowski and Raven 1997) were measured by applying a series of nine increasing actinic irradiances (duration 20 s) and determining the quantum yield of photosynthesis (Φ_p) for each irradiance increment using the PAM fluorometer. Electron transport rate (ETR), a proxy for the light reactions of photosynthesis (Falkowski and Raven 1997) was estimated using the general formula

$$\text{ETR} = \Phi_p \times E \times 0.5 \times A \quad (4)$$

where E is the calibrated PAR from the PAM fluorometer and A is the absorptance. Because frond absorptance data were not collected, we used the default value of 0.84 to calculate the relative ETR. Maximal ETR, the slope of light-dependent ETR (α), and the derived light saturation parameter (E_k) were modeled from the resultant light curves using the following standard negative exponential equation (Falkowski and Raven 1997):

$$\text{ETR} = \text{ETR}_{\max} [1 - (e^{-\alpha E : \text{ETR}_{\max}})] \quad (5)$$

and

$$E_k = \text{ETR}_{\max} : \alpha \quad (6)$$

A photoinhibition term was not included because raw data did not exhibit decreased ETR at high irradiance and models failed to converge if the parameter was included. Parameters were estimated using the *nlinfit* function in Matlab (2007 version), which provides least squares parameter estimates using the Gauss-Newton algorithm with Levenberg-Marquardt modifications for global con-

vergence. Linearity was assessed by investigating the residuals of the observed and fitted responses. Because of potential inter-site and interindividual differences in absorptance, only E_k values were statistically compared between sites, because this parameter is not sensitive to variations in absorptances. E_k values were then compared to ambient PAR levels typical of the two sites, the subsequent reduction in PAR afforded by experimental shades, and the natural attenuation during periods of immersion under high phytoplankton biomass.

Environmental measurements—Local processes can lead to differences in total irradiance and phytoplankton biomass in the water column, subsequently affecting the growth of *S. sessile*. Chl *a* was extracted from bottle samples taken from the surf zone (Menge et al. 1997, 2008); because sampling frequency varied between sites and between years, only monthly means (\pm SEM) are reported. Eight-day composites of SeaWiFS-derived PAR were downloaded for the pixel nearest to each of the sites. Because of the timescale mismatch between the PAR data and tidal cycles, we could compare PAR differences only between sites and not directly to kelp growth. We attempted to measure PAR directly using sensors installed in the lower intertidal and supralittoral zones at both sites, but three of the four sensors failed within 3 weeks of deployment so no useful data were available for this study.

To quantify sediment content in water flowing over the plots, we installed mesh-enclosed sponges, Dobies®, at each experimental block at both sites. Dobies were collected and replaced every 2 weeks throughout the duration of the experiment. The sponges were thoroughly rinsed over a 53- μ m sieve, capturing larger organic particulates and sand, thus providing a relative means of comparing between sites. Samples were dried at 67°C for 2 d, weighed, combusted at 400°C in a muffle furnace, and reweighed to estimate the sand and organic content of each sample. We also measured sediment accumulation in the plots by visual estimates of percentage cover (Dethier et al. 1993).

Variability in nutrient availability and temperature at different scales can lead to differences in growth among treatments and between sites. Data regarding upwelling strength (Bakun Index) were downloaded from the National Oceanic and Atmospheric Administration's Pacific Fisheries Environmental Laboratory (<http://pfel.noaa.gov>), binned into 2-week means for the period prior to growth measurement, and compared to growth rates of unmanipulated *S. sessile* fronds across both sites. Because of the coarse spatial nature of the Bakun Index, site-level variability could not be resolved. To quantify water flow in the plots, we used dental chalk flow blocks (Doty 1971). The chalk blocks were deployed in the center of shaded and unshaded treatments at both sites simultaneously four times during the season. Dry weight loss during the deployment provided an estimate of relative flow. In situ temperature was recorded with Hobo Stowaway underwater temperature loggers attached to the rock near the plot in stainless steel housings. The loggers thus provided estimates of both air temperature (at low tide) and water temperature (at high tide). Plot slope, which could

Table 2. Spatiotemporal relationships of phytoplankton abundances and benthic macrophyte abundances in upwelling-dominated regions along the U.S. west coast. Phytoplankton standing stock was assessed using nearest pixel SeaWiFS 9-km summer averages for standard Chl *a* product (space) or May–July averages derived from 8-d standard Chl *a* product (time). Data in spatial comparisons were from summer 2002 and spanned the region of 35–46°N. Temporal analyses compared nearshore phytoplankton abundances to macrophyte abundance at Strawberry Hill (SH) and Fogarty Creek (FC) for 2000–2004. All results follow the following general formula: benthic macrophyte abundance (% cover) = slope × nearshore Chl *a* (mg m⁻³) + intercept. Values significant at $p < 0.05$ are in boldface.

	Slope	Intercept	R^2 (adjusted)	<i>n</i>	<i>F</i>	<i>p</i>
Space						
35–46°N	-3.33	159	0.56	20	25.1	0.001
39–46°N	-3.75	157	0.72	15	36.3	0.0001
Time						
SH (44.23°N)	-2.00	122	0.78	5	15.1	0.03
FC (44.83°N)	-6.66	178	0.12	5	4.28	0.301

confound both the effects of light and temperature, was estimated using an inclinometer, with accuracy to $\pm 3^\circ$.

Statistical analysis—In order to test the hypothesis that bloom-equivalent light regimes could limit kelp growth, we used a multifactor repeated measures analysis of variance (rmANOVA; Anderson 1978) to determine the relative magnitude and persistence of the effects of shading and site on the growth rate of *S. sessile*. Because the manipulation control was added in mid-June, time periods considered for repeated measures were subsequent to this treatment addition. For all analyses, the more conservative multivariate approach was used. To test the effect of shading on accumulated algal abundance across treatments and between sites, defined as the difference between initial and final percentage cover of *S. sessile* (mid-June to end of August 2004), we used analysis of variance (ANOVA).

To account for effects of non-manipulated physical factors, we tested for site and treatment differences in plot slope, mean flow, sediment accumulation, organic matter accumulation, and water column Chl *a* concentrations (bottle samples) using ANOVA. We used paired *t*-tests to test for between-site differences in mean daily water and air temperatures, mean daily temperature maxima, mean daily temperature range, 8-d SeaWiFS-derived PAR, and 8-d SeaWiFS-derived Chl *a*. We used a mixed forward and backward stepwise multiple linear regression to determine the relative effect size on *S. sessile* growth rates of treatment, site, site × treatment interaction, slope, sediment accumulation, organic matter accumulation, and mean percentage cover of sand (visually estimated in 0.25-m² quadrats). Explanatory variables were sequentially added and removed with $p(\text{include}) = p(\text{exclude}) = 0.25$. The best fit model was determined by maximizing the adjusted R^2 and minimizing the Akaike Information Criterion (AIC). All statistical analyses were performed using JMP V.4 and SAS V.8.1 software.

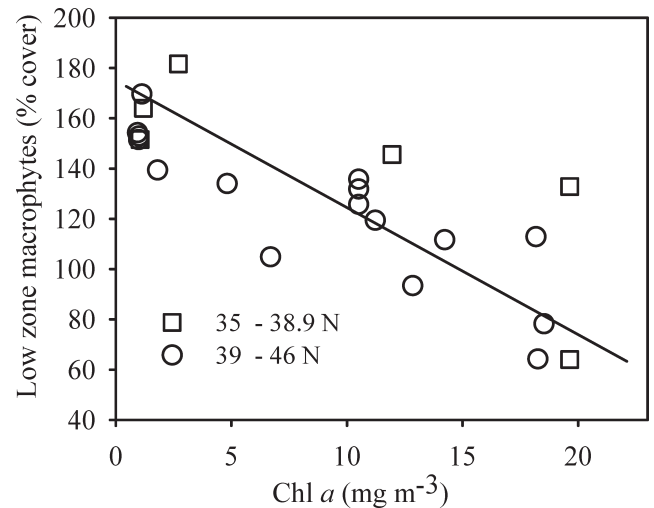


Fig. 2. Regional correlation of SeaWiFS derived summer Chl *a* concentrations and benthic macrophyte abundances in wave-exposed low rocky intertidal zones.

Results

Spatiotemporal context—Across sites ranging from 35°N to 48°N, low-zone macrophyte abundance and nearshore phytoplankton abundance (satellite-derived Chl *a*) were negatively correlated (Table 2; Fig. 2; $p < 0.001$). However, considering only northern California (Cape Mendocino) to Oregon (39–46°N), the relationship was much stronger (Table 2). Thus, Chl *a* concentrations greater than ~ 15 mg m⁻³ were associated with low-zone macroalgal covers of less than 100% (Fig. 2; Table 2). Because of land-masking and increased incidence of clouds, the nearest pixel assessed for Chl *a* could be ~ 9 km offshore; concentrations over intertidal and subtidal reefs are probably higher (Menge et al. 1997).

Temporal shifts in the abundances of pelagic and benthic primary producers may be site-specific (Table 2, Fig. 3). Satellite-derived Chl *a* concentrations were higher off of SH during the years 2001–2003 than in previous or subsequent years (Fig. 3). Site-level macrophyte abundances sharply decreased at both sites over the period of observation, and the apparent recovery at SH in 2004 was matched by a concurrent drop in nearshore Chl *a* concentrations (Fig. 3; Table 2). At SH, an increase of 11.2 mg m⁻³ Chl *a* was associated with a decrease from 122% to less than 100% cover of low zone algae. The interannual pattern was less apparent off FC; although macrophytes did decline at this site from 2000–2002 (Fig. 3), this was not correlated with Chl *a* concentrations (Table 2).

Phytoplankton effects on the intertidal light environment—According to our modeled relationship, only 20% of surface irradiance is available at the mean depth of *S. sessile* with 20 mg Chl *a* m⁻³ in the water column (Fig. 4). At this concentration of Chl *a* the resultant transmissivity is less than even that of the experimental shades (25–40%). Using the smaller k_c from Kirk (1994), the experimental

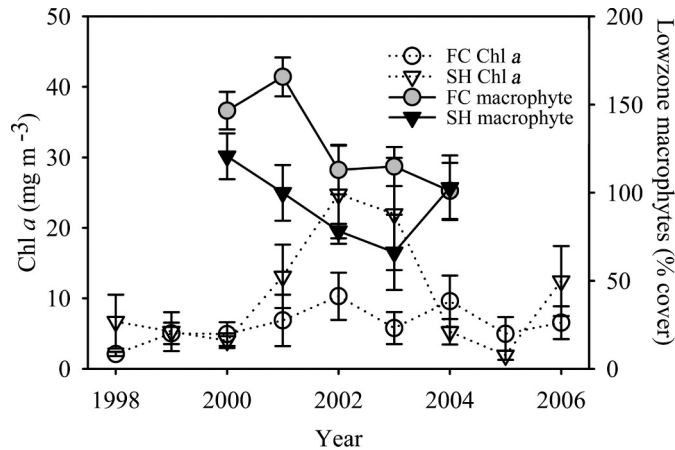


Fig. 3. Temporal patterns of SeaWiFS-derived Chl *a* concentrations and benthic macrophyte abundances for SH and FC.

shading was ecologically relevant at pigment concentrations greater than $60 \text{ mg Chl } a \text{ m}^{-3}$, which still occurred frequently (Fig. 5).

Surf-zone Chl *a* concentrations (from shore-based samples of extracted Chl *a*) were much lower in 2004 than in the previous 3 yr (Fig. 5). From 2001 to 2003, Chl *a* concentrations in the surf zone had summer peaks in July and August, reaching maxima between 55 and $110 \text{ mg Chl } a \text{ m}^{-3}$ at SH and less than $20 \text{ mg Chl } a \text{ m}^{-3}$ at FC. In 2004, concentrations were much less than in previous years, and site-level differences were weakly reversed (Figs. 3, 5; $\text{SH}_{\text{max}} = 26 \text{ mg Chl } a \text{ m}^{-3}$, $\text{FC}_{\text{max}} = 53 \text{ mg Chl } a \text{ m}^{-3}$). Satellite-derived Chl *a* concentrations were also low and did not differ between sites that year (Table 3). Considering only years with sampling frequency greater than one per month (2002–2004), nearshore (satellite-derived) and surf-

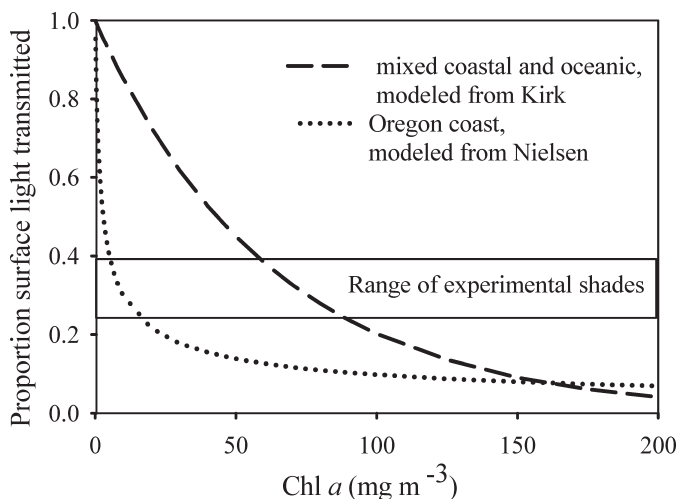


Fig. 4. Transmissivity with varying modeled pigment concentration comparing the effect of two different values for the specific Chl *a* attenuation, k_c : this study and Kirk (1994). The range of transmissivity afforded by experimental shades is overlaid. Experimental plots were approximately 1 m below mean sea level.

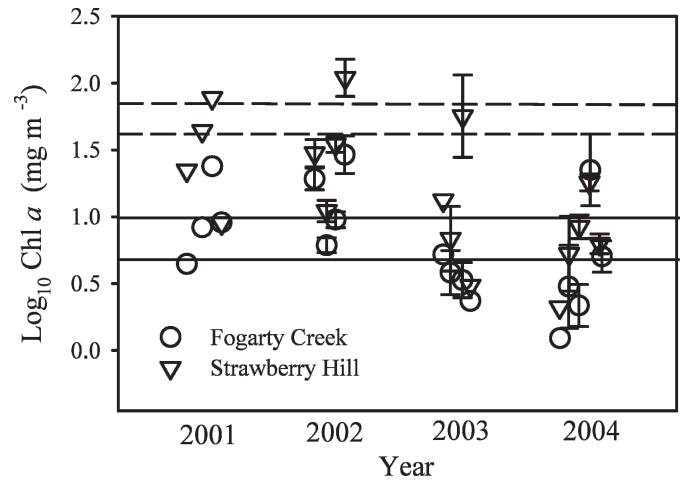


Fig. 5. Mean surf-zone Chl *a* concentrations (\pm SEM) extracted from bottle samples along the central Oregon coast during May–August of 2001–2004. Horizontal lines represent the Chl *a* equivalents of experimental shades as defined in Figure 4.

zone (extracted) Chl *a* concentrations were positively correlated on coarse time scales (sites pooled, May–July averages; mean extracted $[\text{Chl } a] = -1.88 + 1.29 \times [\text{mean satellite-derived } [\text{Chl } a]]$; $R^2 = 0.75$, $F_{1,5} = 15.93$, $p = 0.016$).

Comparing the absorption of *S. sessile*, a common coastal diatom, and a mixed nearshore phytoplankton assemblage revealed near-complete spectral overlap (Fig. 6). The light available to kelps would be determined by the spectrally weighted absorption of the phytoplankton in the overlying water column. High phytoplankton abundance along the Oregon coast therefore would diminish the total quantity of light to the benthos and specifically in the wavelengths that the kelp most readily utilizes.

Physical characteristics—Ambient PAR (as derived by the SeaWiFS sensor) was slightly higher at SH than at FC for the duration of the study (Table 3). Sand accumulation was several times greater at SH than at FC (Table 3). Particulate organic matter did not differ between the two sites (Table 3). Visual estimates of percentage cover of sand in experimental plots revealed a pattern similar to that occurring in collectors; sand covered more space in plots at SH than at FC (rmANOVA 5–6% at SH compared to 0 at FC, $p < 0.05$).

Because of the coarse spatial resolution of the wind-derived indices, upwelling differences between sites could not be resolved. Mean growth rate (pooled across sites) was positively correlated with upwelling through time ($\text{cm d}^{-1} = 0.087 \text{ m}^3 \text{ s}^{-1} 100 \text{ m}^{-1} + 0.007 \text{ cm d}^{-1}$; $R^2 = 0.77$, $F_{1,5} = 18.4$, $p = 0.013$). However, autocorrelation could not be assessed with such a short time series ($t = 6$), and thus the degrees of freedom and the power of the relationship were likely inflated (Chatfield, 2004).

Chalk dissolution rates were slightly higher beneath the shades when averaged across both sites and through all

Table 3. Differences in site-level physical parameters. Values represent grand means (number of replicates in parentheses). Boldface values are significantly different from each other at the $p < 0.05$ level. Slope is represented by vertical degrees. Flow is represented by the mean change in mass of in situ chalk blocks because of erosion. Sand and organic matter are represented by the mean mass deposited in Dobbie collectors. Emerged and immersed temperatures are a result of detiding the same Hobo tidbit. Sea-viewing Wide Field-of-view Sensor (SeaWiFS)-derived chlorophyll *a* (Chl *a*) and photosynthetically active radiation (PAR) are 8-d composites from the nearest pixel to the intertidal site.

	Fogarty Creek	Strawberry Hill	<i>t</i> statistic
Slope (degrees; $n=30$)	13	16.5	1.67
Flow (g lost; $n=20$)	1.93	1.85	1.15
Sand in collectors (g; $n=10$)	0.96	5.86	10.63
Organic matter in collectors (g; $n=10$)	0.073	0.075	0.343
Daily avg. temp. emerged ($^{\circ}\text{C}$; 01 Jun–30 Jul 2004; $n=40$)	12.37	13.45	4.16
Daily avg. temp. immersed ($^{\circ}\text{C}$; 01 Jun–30 Jul 2004; $n=60$)	10.91	11.17	2.08
Daily avg. temp. ($^{\circ}\text{C}$; 01 Jun–30 Jul 2004; $n=60$)	11.09	11.33	2.30
SeaWiFS-derived Chl <i>a</i> (mg m^{-3} ; 20 May–30 Jul 2004; $n=10$)	11.6	8.25	1.21
SeaWiFS-derived PAR ($\text{mol m}^{-2} \text{d}^{-1}$; 20 May–30 Jul 2004; $n=10$)	50	53	4.81

measurements in time ($-$ shade = 1.79 g, $+$ shade = 1.98 g, $F_{1,73} = 4.47$, $p = 0.04$). This slight but real difference could be because of a “chute” effect, or channeling of the water volume beneath the experimental shade. Dissolution rates did not differ between sites or between treatments within sites (Table 3). Mean air temperature was 1.2°C higher at SH than at FC (Table 3) and mean water temperature was marginally warmer (0.25°C). Plot slope did not differ between sites or treatments (Table 3).

Experimental results—Effect of shading: *S. sessile* growth rate was less in the $+$ shade treatment than in either of the control plots ($-$ shade and manipulation control; Fig. 7). Growth of *S. sessile* was context-dependent (Table 4; between-subjects site \times shade interaction) with the shade effect being stronger at SH than at FC (Fig. 7). Repeated measures ANOVA revealed no differences in growth rates of unshaded *S.*

sessile between sites (Table 4). The strength of the shading effect also varied through time (Table 4; within-subjects time \times shade interaction) with the greatest effect being in mid- and late July 2004 (Fig. 7). *S. sessile* growth rate did not differ between the two control treatments ($-$ shade and manipulation control; Table 5), though the effect of each control varied through time (Table 5, within-subjects time \times treatment interaction).

The effects of shading on percentage cover of *S. sessile* were similar to those on growth. Together, shade, site, and shade \times site interaction explained over half of the variance in percentage cover of *S. sessile* (ANOVA, $R^2 = 0.52$, $F_{3,26} = 9.4$, $p < 0.001$). Across sites, unshaded plots increased in cover more than shaded (Fig. 8; shade effect = -16.7% ; ANOVA, $F_{1,26} = 14.6$, $p < 0.001$) and overall increases in relative abundances were less (or actually decreased) at FC (site effect = -7.4% , $F_{1,26} = 13.6$, $p < 0.001$). The effect of shade on cover did not vary with site ($F_{1,26} = 0.09$, $p = 0.76$). Surveys prior to the initiation of the experiment (May 2004) revealed no differences in relative abundances of *S. sessile* between sites (mean percentage cover \pm 95% confidence interval [CI]: FC = $44 \pm 16\%$, SH = $53 \pm 13.8\%$; $F_{1,18} = 0.92$, $p = 0.35$) or in the densities of thalli between sites (mean individuals $\text{m}^{-2} \pm$ 95% CI: FC = 28.4 ± 5.4 , SH = 32.5 ± 14.7 ; $F_{1,23} = 0.21$, $p = 0.65$). Because of splitting of blades and merging of haptera-like holdfasts, determining individual sporophytes became difficult; densities were only available for initial conditions.

S. sessile at SH saturated at a higher irradiance than that at FC (SH $E_k = 142.6 \mu\text{mol m}^{-2} \text{s}^{-1} >$ FC $E_k = 86 \mu\text{mol m}^{-2} \text{s}^{-1}$; ANOVA, $F_{1,8} = 14.3$, $p = 0.0069$). Less-than-saturating irradiances occurred beneath the experimental shades as well as during periods of high plankton biomass (Fig. 9). Because of the length of dark acclimation, we recognize that these E_k values may be substantially lower than what would occur later in a diel cycle (e.g., Nielsen et al. 2006).

Influence of other factors: Using grand means of *S. sessile* growth rates across all measurements in time ($n =$

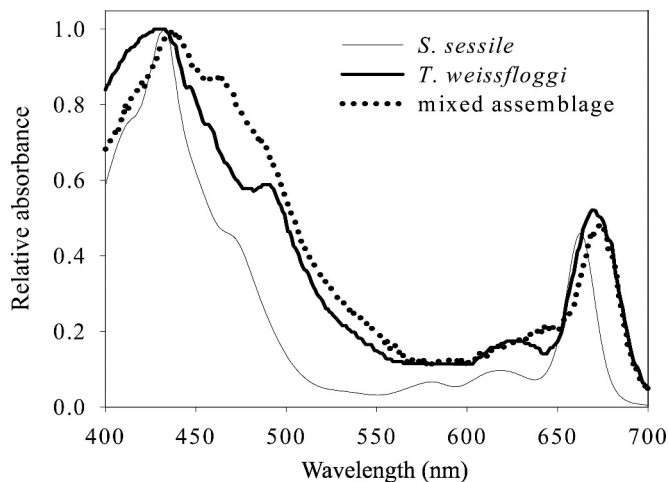


Fig. 6. The relative PAR absorbance capacity of the intertidal kelp *S. sessile* as compared to a common nearshore diatom and a nearshore mixed assemblage of phytoplankton. Absorbances are normalized to individual maxima to account for differences in biomass.

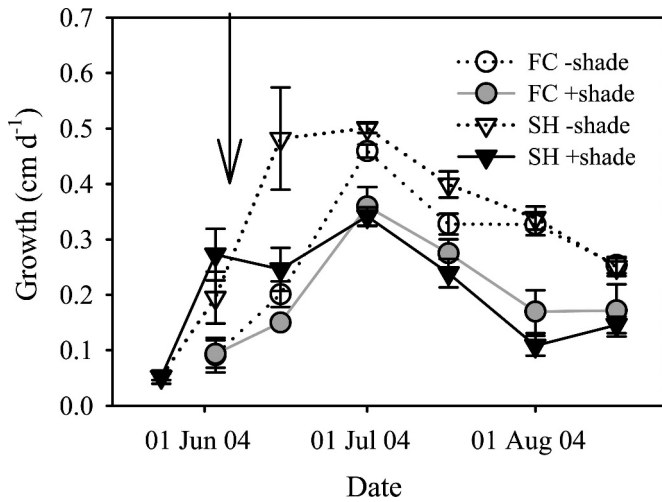


Fig. 7. Effect of shading on *S. sessile* growth, May–August 2004. Growth rates (\pm SEM) are shown for *S. sessile* in two treatments: shaded (+shade, +trim) and control (–shade, +trim). Because no difference was found between shade control and manipulation control, the latter is omitted for clarity. The arrow denotes the period when shades were installed.

30), three explanatory variables (shading, trimming, and site) remained after forward and backward stepwise regression (Table 6). Variables eliminated included slope, mean organic matter, and mean percentage cover of sand. A 60–75% reduction in downward irradiance led to a mean decrease in growth rate of approximately 25% overall (Table 6; mean growth rate = 0.32 cm d^{-1} ; mean shade effect = -0.078 cm d^{-1}) and accounted for over 72% of the variance in growth of *S. sessile* (Table 6; “reduced” model, shade only; $R^2 = 0.72$). Trimming, after accounting for the shade effect, still had a negative effect on mean growth rate, although its magnitude was approximately one third that of shading (Table 6; trim effect = -0.027). Finally, in contrast to rMANOVA, the stepwise linear regression revealed that overall growth rates at FC were approximately 0.06 cm d^{-1} less than at SH after accounting for shading, trimming, and the site \times shade interaction (Table 6; $p < 0.01$). These additional variables, however, contributed only an additional 10% of the variance explained compared to the reduced model of shade only (Table 6). Furthermore, several eliminated variables (i.e., sediment and slope) covary with site. When site was not included in the initial model, only shading remained as an explanatory variable ($R^2 = 0.72$, $F_{1,26} = 90.6$, $p < 0.001$).

Discussion

General patterns—Increased phytoplankton abundance was associated with decreased benthic macroalgal abundance in regions dominated by upwelling along the U.S. west coast. The pattern was enhanced for the regions spanning 39–46°N. In the summer of 2002, during a period of atypically high phytoplankton biomass (Thomas et al. 2003), over 70% of the observed variance in site-level macrophyte abundance was explained by nearshore Chl *a* concentrations. This result is in agreement with the

Table 4. Repeated measures multivariate ANOVA: Effect of shade and site on growth of *S. sessile* (cm d^{-1}). MS=mean square, $\text{Prob}>F$ =the probability that differences are due to chance. Boldface values denote statistically significant difference at the $p < 0.05$ level.

Source of variation	MS	Exact <i>F</i>	df	Prob> <i>F</i>
Between subjects				
Shade	4.14	103	1	<0.0001
Site	0.011	0.280	1	0.602
Site \times shade	0.212	5.30	1	0.03
Error	0.040		25	
Within-subjects multivariate				
Time	1.92	14.8	3	<0.0001
Time \times shade	0.91	7.02	3	0.0016
Time \times site	0.29	2.23	3	0.112
Time \times site \times shade	0.058	0.45	3	0.720
Error	0.130		23	

negative correlation at local scales documented for SeaWiFS-derived Chl *a* and the kelp *Macrocystis* (Broitman and Kinlan 2006). At SH (44.23°N), the pattern was also apparent through time, with high phytoplankton abundances associated with decreased macrophyte abundances and recovery when phytoplankton abundances were atypically low (2004). This temporal pattern was not evident at FC (44.83°N), which may be expected in a region with a narrower shelf and likely less phytoplankton retention.

Satellite-derived Chl *a* concentrations in excess of 15.2 mg m^{-3} regionally and 11.2 mg m^{-3} for SH were associated with macroalgal covers of less than 100%. For a given algal-dominated stretch of coastline, this reduction is analogous to a shift from a multilayered canopy to one with a single layer or to a patch with open spaces where sessile invertebrates can recruit. In addition to changing the light environment, high phytoplankton abundance also favors the growth of sessile invertebrates (Sanford and Menge 2001; Menge et al. 2008), which are considered to be better competitors for space than

Table 5. Repeated measures multivariate ANOVA: effect of control treatments and site on growth of *S. sessile* (cm d^{-1}). Treatments include control (–artificial shade, +trim), and trim control (–artificial shade, –trim). MS=mean square, $\text{Prob}>F$ =the probability that differences are due to chance. Boldface values denote difference at the $p < 0.05$ level.

Source of variation	MS	Exact <i>F</i>	df	Prob> <i>F</i>
Between subjects (all between, NS)				
Site	0.24	3.65	1	0.08
Treatment	0.16	2.42	1	0.14
Site \times treatment	0.00009	0.001	1	0.97
Error	0.062		15	
Within subjects multivariate (all within, $p < 0.001$)				
Time	5.60	24.4	3	<0.0001
Time \times site	0.90	3.90	3	0.08
Time \times treatment	4.90	21.1	3	<0.0001
Time \times site \times treatment	0.55	2.38	3	0.12
Error	0.214		13	

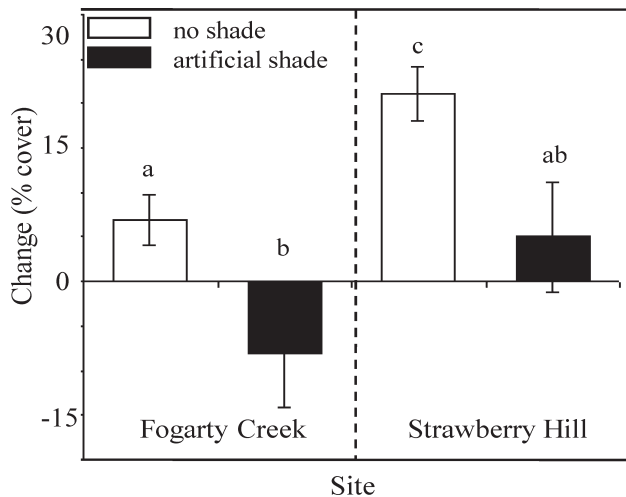


Fig. 8. Differences in changes in percentage cover of *S. sessile* in plots with and without shading. For this analysis the -shade control and manipulation control plots were pooled: (+shade) = 5 plots per site; (-shade) = 10 plots per site. Means with distinct letters are statistically different (ANOVA, $p < 0.05$).

macroalgae in mid- and low-zone environments (Lubchenco and Menge 1978). However, although the temporal and spatial patterns of satellite-derived and surf-zone Chl *a* are similar at seasonal time scales, the degree of cross-shelf coherence at shorter timescales is as yet unknown. Furthermore, field experiments that explicitly and concurrently test the relative importance of competition with invertebrates for space and modification of the

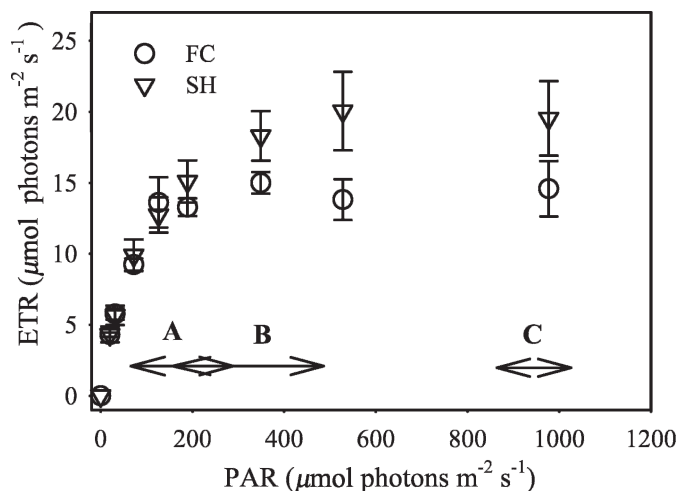


Fig. 9. Electron transport rate (ETR) of *S. sessile* with increased irradiance. Blades were removed from manipulation control at the end of the experiment (mid-September 2004); $n = 5$ blades per site. Responses from blades from Strawberry Hill (SH) are denoted by triangles, those from Fogarty Creek (FC) by circles; ETR values have not been biomass-adjusted. Horizontal arrows denote irradiances of interest discussed in text: (A) available PAR during immersion, (B) the fraction of (A) that was available with experimental shades, and (C) mean daily instantaneous PAR for June and July along the central Oregon coast.

Table 6. Best fit model from a stepwise regression on all observed explanatory variables on *S. sessile* growth rate. Best fit was determined with mixed (forward and backward) stepwise multiple linear regression. Parameter inclusion and exclusion were determined by $p_{(\text{enter/leave})}=0.25$ and subsequently those that maximized adjusted R^2 and minimized the AIC (see text). The resulting model retained shade, trimming, and site (indicated in boldface type) as major effects: adjusted $R^2=0.82$, $p<0.0001$, $F_{5,29}=27.5$. Reduced model: shade effect only, $R^2=0.72$, $p<0.001$, $F_{1,26}=90.6$. Prob>|t|=the probability that differences are due to chance. Boldface effect estimates and probabilities denote $p<0.05$. See text for initial list of explanatory variables.

Parameter	Estimate	SE	<i>t</i> ratio	Prob> <i>t</i>
Intercept	0.320	0.006	51.1	<0.0001
Shade effect (shaded-control and trim control)	-0.073	0.007	-11.0	<0.0001
Trim effect (control-trim control)	-0.020	0.008	-2.84	0.01
FC*	-0.019	0.007	-2.9	0.008
Shade effect ×FC	0.018	0.007	2.8	0.01

* FC, Fogarty Creek.

light environment by phytoplankton have yet to be completed. Nevertheless, these results suggest that the paradigm of invertebrates as competitive dominants along rocky shores may be context-dependent.

The magnitude, frequency, and spectral quality of blooms along the central Oregon coast evidently can contribute to light-limiting conditions for *S. sessile*. According to our modeled transmissivities, Chl *a* concentrations ranging from only 20 to 60 mg m^{-3} are equivalent to shading generated by experimental shades and are thus sufficient to limit the growth and relative abundance of this intertidal kelp. These concentrations occur quite frequently along the central Oregon coast. Experimental shades were spectrally neutral, whereas the high degree of spectral overlap between *S. sessile* and the overlying phytoplankton assemblage suggests spectrally competitive absorbances. The experimental shades were therefore a conservative mimic of the reduction in light intensity and spectral quality that occurs during blooms and may actually underestimate the true effect of blooms on kelp growth.

Effect of shading—Over the course of our 3.5-month study, decreasing PAR to bloom-equivalent levels led to a 25% reduction in growth rate of *S. sessile*, accounted for over 72% of the variance in growth, and led to decreases in relative abundances of the intertidal kelp. Growth rates beneath the shades remained depressed for the duration of the field experiment, suggesting that the effects of shade could not be overcome by acclimation. Although the magnitude of the effect varied between sites, suggesting physiological complexity or context dependency in the response, overall the results are clear. Bloom-equivalent light levels are sufficient to adversely affect an ecologically dominant intertidal kelp, and such light-limiting conditions occur frequently along the Oregon coast with likely ecosystem-level consequences.

Exogenous factors such as water flow (Hurd 2000) and temperature (e.g., Tegner et al. 1997), as well as endogenous factors such as nutrient uptake rates and storage capacity (e.g., Korb and Gerard 2000) and acclimation and local adaptation to light history (e.g., Herbert and Waaland 1987), can change the effect of light on growth rates, leading to context dependency of responses to decreased light. The shading effect was more dramatic at SH (site \times shade effect; Tables 4 and 6), leading to a larger difference in frond elongation rates between the control and shaded plots at that site. Although internal nutrient stores were not quantified, external nutrient concentrations did not differ between sites (nitrate + nitrite, mean \pm SD: FC = $12.19 \pm 5.35 \mu\text{mol L}^{-1}$, SH = $5.41 \pm 4.67 \mu\text{mol L}^{-1}$; F. T. Chan unpubl. data) nor did flow rates. Air temperatures were 1.2°C higher at SH, but temperatures during immersion were only 0.25°C higher (Table 3). SeaWiFS-derived PAR levels were also higher at SH for the duration of the experiment (Table 3). It is likely that the difference in growth rates and the response to shading between sites was caused by differences in ambient PAR or a combined temperature–light effect.

Saturation irradiances of *S. sessile* were higher for fronds from SH (Fig. 9), suggesting that seasonal acclimation may have played a role. All factors being equal, sun-acclimated populations would have increased growth rates in higher light than shade-acclimated populations. In low light, such as that provided by experimental shades and midsummer phytoplankton blooms, they would be expected to respond more adversely. Controlled experiments conducted in spring and early summer in concert with explicit physiological studies should illuminate the context dependency of the shading response and whether it occurs as a result of seasonal acclimation or other endogenous factors.

The potential for light–nutrient co-limitation in this system should not be ignored. Growth of *S. sessile* varied through time (Fig. 7), reaching a peak in early July. Although growth of fronds was positively correlated with upwelling, increases in growth rate may have also been a function of seasonal increases in ambient PAR, which reached its peak in late June and early July. These temporal patterns occurred in a year when phytoplankton abundances were atypically low and thus competition for upwelled nutrients with phytoplankton would have been diminished. Longer-term monitoring of macrophyte growth rates over a larger spatial scale should help to determine the role of upwelling dynamics in structuring benthic- or pelagic-based biomass of primary producers.

Photosynthesis of *S. sessile* may be severely curtailed by carbon limitation during emersion, as has been found for other phaeophytes (Williams and Dethier 2005); to date carbon limitation during emersion has not been explicitly tested for *S. sessile*. Our experimental shades were a conservative approximation of light availability considering both immersion and emersion periods. If *S. sessile* is carbon-limited during emersion, much lower concentrations of phytoplankton are necessary to produce the same result because there will be little compensation during emersion.

This study provides the first evidence that phytoplankton can limit the light availability to benthic macrophytes in energetic open-coast systems, extending the theoretical and experimental findings of estuarine and lacustrine studies. Furthermore, if recent increases in nearshore phytoplankton abundance (Kahru and Mitchell 2008) are symptomatic of an oceanic regime shift (Bond et al. 2003; Peterson and Schwing 2003), we speculate that the resulting increased attenuation of light by phytoplankton will lead to profound changes in benthic communities. Ultimately, longer-term monitoring in the low intertidal and sublittoral zones at a larger spatial scale will be necessary to determine the effect of oceanic regime shift on upwelling, nearshore phytoplankton production, macroalgal ecophysiological dynamics, and the extent of coupling between these three processes. Nevertheless, the large-scale observations and experimental results in our study suggest that light limitation might be important even in intertidal environments where the deepest level of immersion is only about 3 m.

References

- ANDERSON, T. W. 1978. Repeated measurements on autoregressive processes. *J. Am. Stat. Assoc.* **73**: 371–378.
- ARMSTRONG, S. L. 1989. The behavior in flow of the morphologically variable seaweed, *Hedophyllum sessile* (C. Ag) Setchell. *Hydrobiologica* **183**: 115–122.
- BOND, N. A., J. E. OVERLAND, M. SPILLANE, AND P. STABENO. 2003. Recent shifts in the state of the North Pacific. *Geophys. Res. Lett.* **30**: 2183, doi:10.1029/2003GL018597.
- BORUM, J., AND K. SAND-JENSEN. 1996. Is total primary production in shallow coastal marine waters stimulated by nitrogen loading? *Oikos* **16**: 406–410.
- BOYD, P. W., AND S. C. DONEY. 2002. Modelling regional responses by marine pelagic ecosystems to global climate change. *Geophys. Res. Lett.* **29**: 1806, doi:10.1029/2001GL014130.
- BROITMAN, B. R., AND B. P. KINLAN. 2006. Spatial scales of benthic and pelagic producer biomass in a coastal upwelling ecosystem. *Mar. Ecol. Prog. Ser.* **327**: 15–25.
- BURNAFORD, J. L. 2004. Habitat modification and refuge from sublethal stress drive a marine plant-herbivore association. *Ecology* **85**: 2837–2849.
- BUSTAMANTE, R. H., AND OTHERS. 1995. Gradients of intertidal primary productivity around the coast of South Africa and their relationships with consumer biomass. *Oecologia* **102**: 189–201.
- CHATFIELD, C. 2004. The analysis of time series. Chapman and Hall.
- DAYTON, P. K. 1985. The ecology of kelp communities. *Annu. Rev. Ecol. Syst.* **16**: 215–245.
- DETHIER, M. N., E. S. GRAHAM, S. COHEN, AND L. M. TEAR. 1993. Visual versus random-point percent cover estimations: 'Objective' is not always better. *Mar. Ecol. Prog. Ser.* **110**: 9–18.
- DOTY, M. S. 1971. Measurement of water movement in reference to benthic algal growth. *Bot. Mar.* **14**: 32–35.
- DRING, M. 1987. Light climate in intertidal and subtidal zones in relation to photosynthesis and growth of benthic algae: A theoretical model. p. 22–34. *In* R. M. M. Crawford [ed.], *Plant life in aquatic and amphibious habitats*. Blackwell, Oxford.

- FALKOWSKI, P. G., AND J. A. RAVEN. 1997. Aquatic photosynthesis. Blackwell Science.
- GENTY, B., J. BRIANTAIS, AND N. BAKER. 1989. The relationship between quantum yield of photosynthetic electron transport and the quenching of chlorophyll fluorescence. *Biochim. Biophys. Acta* **990**: 87–92.
- GRANTHAM, B. A., AND OTHERS. 2004. Upwelling-driven nearshore hypoxia signals ecosystem and oceanographic changes in the northeast Pacific. *Nature* **429**: 749–754.
- HALPIN, P. A., P. T. STRUB, B. PETERSON, AND T. BAUMGARTNER. 2004. An overview of interactions among oceanography, marine ecosystems, climatic and human disruptions along the eastern margins of the Pacific Ocean. *Rev. Chil. Hist. Nat.* **77**: 371–409.
- HARLEY, C. D. G. 2002. Light availability indirectly limits herbivore growth and abundance in a high rocky intertidal community during the winter. *Limnol. Oceanogr.* **47**: 1217–1222.
- HERBERT, S. K., AND J. R. WAALAND. 1987. Photoinhibition of photosynthesis in a sun and shade species of the red alga *Porphyra*. *Mar. Biol.* **97**: 1–7.
- HURD, C. L. 2000. Water motion, marine macroalgal physiology, and production. *J. Phycol.* **36**: 453–472.
- JUSTIC, D., N. N. RABALAIS, AND R. E. TURNER. 1996. Effects of climate change on hypoxia in coastal waters: A doubled CO₂ scenario for the northern Gulf of Mexico. *Limnol. Oceanogr.* **41**: 992–1003.
- JONES, C. G., J. H. LAWTON, AND M. SHACHAK. 1994. Organisms as ecosystem engineers. *Oikos* **69**: 373–386.
- KAHRU, M., AND G. B. MITCHELL. 2008. Ocean color reveals increased blooms in various parts of the world. *EOS Trans.* **89**: 170.
- KAIN, J. M. 1976. The biology of *Laminaria hyperborea* IX. Growth pattern of fronds. *J. Mar. Biol. Assoc. U.K.* **56**: 603–628.
- KIRINCICH, A. R., J. A. BARTH, B. A. GRANTHAM, B. A. MENGE, AND J. LUBCHENCO. 2005. Wind-driven inner-shelf circulation off central Oregon during summer. *J. Geophys. Res.* **110**: C10S03, doi:10.1029/2004JC002611.
- KIRK, J. 1994. Light and photosynthesis in aquatic ecosystems. Cambridge Univ. Press.
- KORB, R. E., AND V. A. GERARD. 2000. Nitrogen assimilation characteristics of polar seaweeds from differing nutrient environments. *Mar. Ecol. Prog. Ser.* **198**: 83–92.
- KRAUSE-JENSEN, D., AND K. SAND-JENSEN. 1998. Light attenuation and productivity of aquatic plant communities. *Limnol. Oceanogr.* **43**: 396–407.
- LANE, C. E., C. MAYS, L. D. DRUEHL, AND G. W. SAUNDERS. 2006. A multi-gene molecular investigation of the kelp (*Laminariales*, *Phaeophyceae*) supports substantial taxonomic reorganization. *J. Phycol.* **42**: 493–512.
- LARKUM, A. W. D. 1986. A study of growth and primary production in *Ecklonia radiata* (C. Ag.) J. Agardh (*Laminariales*) at a sheltered site in Port Jackson, New South Wales. *J. Exp. Mar. Biol. Ecol.* **96**: 177–190.
- LAVERY, P. S., R. J. LUKATELICH, AND A. J. McCOMB. 1991. Changes in the biomass and species composition of macroalgae in a eutrophic estuary. *Estuar. Coast. Shelf Sci.* **33**: 1–22.
- LESLIE, H. M., E. N. BRECK, J. LUBCHENCO, AND B. A. MENGE. 2005. Hotspots of barnacle reproduction associated with nearshore ocean conditions. *Proc. Natl. Acad. Sci. USA* **102**: 10534–10539.
- LUBCHENCO, J., AND B. A. MENGE. 1978. Community development and persistence in a low rocky intertidal zone. *Ecol. Monogr.* **48**: 67–94.
- MANN, K. H. 1972. Seaweeds: Their productivity and strategy for growth. *Science* **182**: 975–981.
- MANTUA, N. J., S. R. HARE, Y. ZHANG, J. M. WALLACE, AND R. C. FRANCIS. 1997. A Pacific interdecadal climate oscillation with impacts on salmon production. *Bull. Am. Meteorol. Soc.* **78**: 1069–1079.
- MENGE, B. A., B. A. DALEY, AND P. A. WHEELER. 1996. Control of interaction strength in marine benthic communities, p. 258–274. *In* G. A. Polis and K. O. Winemiller [eds.], *Foodwebs: Integration of patterns and dynamics*. Chapman & Hall.
- , ———, ———, E. DAHLHOFF, E. SANFORD, AND P. T. STRUB. 1997. Benthic-pelagic links and rocky intertidal communities: Bottom-up effects on top-down control? *Proc. Natl. Acad. Sci. USA* **94**: 14530–14535.
- , B. A., F. CHAN, AND J. LUBCHENCO. 2008. Response of a rocky intertidal ecosystem engineer and community dominant to climate change. *Ecol. Lett.* **11**: 151–162.
- MOREL, A. 1988. Optical modeling of the upper ocean in relation to its biogenous matter content (case 1 waters). *J. Geophys. Res.* **93**: 10749–10768.
- NIELSEN, K. J., C. A. BLANCHETTE, B. A. MENGE, AND J. LUBCHENCO. 2006. Physiological snapshots reflect ecological performance of the Sea Palm, *Postesia palmaeformis*, (*Phaeophyceae*) across intertidal elevation and exposure gradients. *J. Phycol.* **42**: 548–559.
- PAINE, R. T. 1984. Ecological determinism in the competition for space: The Robert H. MacArthur Award Lecture. *Ecology* **65**: 1339–1348.
- PETERSON, W. T., AND F. B. SCHWING. 2003. A new climate regime in northeast Pacific ecosystems. *Geophys. Res. Lett.* **30**: 1896, doi:10.1029/2003GL017528.
- PHILLIPS, N. E. 2005. Growth of filter-feeding benthic invertebrates from a region with variable upwelling intensity. *Mar. Ecol. Prog. Ser.* **295**: 79–89.
- SANFORD, E., AND B. A. MENGE. 2001. Spatial and temporal variation in barnacle growth in a coastal upwelling system. *Mar. Ecol. Prog. Ser.* **209**: 143–157.
- SCHOCH, G. C., B. A. MENGE, G. ALLISON, M. KAVANAUGH, S. A. THOMPSON, AND S. A. WOOD. 2006. Fifteen degrees of separation: Latitudinal gradients of rocky intertidal biota along the California Current. *Limnol. Oceanogr.* **51**: 2564–2585.
- SULLIVAN, C. W., A. C. PALMISANO, AND J. B. SOOHOO. 1984. Influence of sea ice and sea ice biota on downwelling irradiance and spectral composition of light in McMurdo Sound, p. 159–165. *In* M. A. Blizard [ed.], *Ocean optics VII*. Proceeding of the Society of Photooptical Instrumentation Engineers, v. 489.
- STENECK, R. S., M. H. GRAHAM, B. J. BOURQUE, D. CORBETT, J. M. ERLANDSON, J. A. ESTES, AND M. J. TEGNER. 2002. Kelp forest ecosystems: Biodiversity, stability, resilience and future. *Environ. Conserv.* **29**: 436–459.
- TEGNER, M. J., P. K. DAYTON, P. B. EDWARDS, AND K. L. RISER. 1997. Large-scale, low-frequency effects on kelp forest succession: A tale of two cohorts. *Mar. Ecol. Prog. Ser.* **146**: 117–134.
- THOMAS, A. C., P. T. STRUB, AND P. BRICKLEY. 2003. Anomalous satellite-measured chlorophyll concentrations in the northern California Current in 2001–2002. *Geophys. Res. Lett.* **30**: 8022, doi:10.1029/2003GL017409.
- TROWBRIDGE, C. D. 1996. Demography and phenology of the intertidal green alga *Codium setchellii*: The enigma of local scarcity on sand-influenced rocky shores. *Mar. Biol.* **127**: 341–351.

- VALIELA, I., J. MCCLELLAND, J. HAUXWELL, P. J. BEHR, D. HERSH, AND K. FOREMAN. 1997. Macroalgal blooms in shallow estuaries: Controls and ecophysiological and ecosystem consequences. *Limnol. Oceanogr.* **42**: 1105–1118.
- WILLIAMS, S. L., AND M. N. DETHIER. 2005. High and dry: Variation in net photosynthesis by the intertidal seaweed, *Fucus gardneri*. *Ecology* **86**: 2373–2379.

Edited by: Anthony Larkum

Received: 14 May 2007

Accepted: 14 July 2008

Amended: 26 August 2008